

## Chronic stress promoted the growth of ovarian carcinoma *via* increasing serum levels of norepinephrine and interleukin-10 and altering nm23 and NDRG1 expression in tumor tissues in nude mice

Guolan Gao<sup>1,#</sup>, Jianling Sun<sup>2,#,\*</sup>, Jun Gao<sup>1</sup>, Lijuan Xiong<sup>1</sup>, Liquan Yu<sup>1</sup>, Yulian Gao<sup>1</sup>

<sup>1</sup> Department of Gynecological Oncology, Aviation General Hospital, Beijing, China;

<sup>2</sup> Department of Cardiology, Aviation General Hospital, Beijing, China.

### Summary

The current study aimed to examine the effects and underlying mechanisms of chronic psychological stress on the growth of ovarian carcinoma. Human ovarian carcinoma cells SKOV-3 were subcutaneously inoculated into nude mice to establish an ectopic mouse model. The animals were experimentally stressed 6 h daily for a total of 42 days with a physical restraint system. We examined the effects of stress on the growth of tumor cells that were inoculated 7 days after the initiation of stress. The growth of SKOV-3 xenografts in the stress group showed a more rapid trend than that in the control. The mean weight of tumors that were removed at the end of the experiment increased by 71.7% in the stress group as compared to the control. In order to explore the underlying mechanisms, we first determined the serum levels of norepinephrine (NE) and interleukin 10 (IL-10) in the mice using an enzyme-linked immunoabsorbent assay (ELISA) and then analyzed protein expression profiles of SKOV-3 xenografts using a proteomics-based approach combining two-dimensional electrophoresis with ultra performance liquid chromatography-electrospray tandem mass spectrometry (nanoUPLC-ESI-MS/MS). Results demonstrated that serum levels of NE and IL-10 were obviously increased in the mice receiving 6 h of immobilization daily for 42 days. In xenografts exposed to stress, a tumor promoting protein nm23 was significantly upregulated while a tumor suppressing protein NDRG1 was obviously downregulated, which were confirmed by subsequent Western blot analysis. Results obtained in the current study suggested that chronic stress promoted the growth of ovarian carcinoma in nude mice through increasing serum levels of NE and IL-10 and altering nm23 and NDRG1 expression in tumor tissues.

**Keywords:** Chronic stress, ovarian carcinoma, norepinephrine, interleukin 10, nm23, NDRG1

### 1. Introduction

Ovarian carcinoma is the second most common gynecologic cancer, with the incidence and mortality of 224,747 and 140,163 cases worldwide in 2008 according to the statistics published by World Health Organization (1). Due to non-specific symptoms in the early stage, approximately two thirds of patients are at the advanced stage of this disease upon diagnosis (2). Thus far, ovarian

carcinoma is still the leading cause of death among gynecological cancers, with overall five-year survival rates of 19-39% (3). Although studies indicated that the initiation and progression of ovarian carcinoma involves alternations or dysregulation of multiple genes and signal transduction pathways (4), factors that drive tumor growth and the underlying mechanisms are not well understood.

Substantial evidence indicated that the onset and progression of cancer is influenced by psychological factors such as stress, and depression as well as social isolation, and adequate psychotherapies are beneficial to cancer patients (5-7). The mechanisms underlying the effects of psychological stress on cancer cells were revealed to be related to the sympathetic nervous system (SNS) and the hypothalamic-pituitary-adrenal (HPA) axis, which further act on the immunological

<sup>#</sup> Both authors contribute equally to this work.

\*Address correspondence to:

Dr. Jianling Sun, Department of Cardiology, Aviation General Hospital, An Ding Men Wai Bei Yuan Road 3, Beijing 100012, China.  
E-mail: sunjianling2000@yahoo.com.cn

system and consequently influence tumor development and prognosis (8). In a previous study, Sood and colleagues demonstrated that chronic stress promoted tumor growth and angiogenesis in a mouse model of ovarian carcinoma *via* activation of the tumor cell cyclic adenosine monophosphate (cAMP)/protein kinase A (PKA) signaling pathway (9). These results suggested psychosocial factors are implicated in the pathologies of ovarian carcinoma and provided clues for possible therapeutic interventions in managing this disease.

In the current study we used a mouse model in which human ovarian carcinoma cells SKOV-3 were subcutaneously inoculated to further illustrate the mechanisms behind the effects of chronic stress on the progression of ovarian carcinoma. From neurochemical and immunological perspectives, we examined alternations of serum levels of norepinephrine (NE) and interleukin-10 (IL-10) in mice exposed to chronic stress. In addition, differential expression of proteins in ovarian cancer tissues were analyzed from the view point of proteomics.

## 2. Materials and Methods

### 2.1. Cell lines and cell culture

The human ovarian cancer cell line, SKOV-3, was obtained from the Institute of Biochemistry and Cell Biology, Shanghai Institute of Biological Sciences, Chinese Academy of Sciences, China. Cells were maintained in RPMI-1640 medium (Thermo Fisher Scientific, Waltham, MA, USA) supplemented with 10% heat-inactivated fetal bovine serum (FBS; Thermo Fisher Scientific) and penicillin-streptomycin (50 U/mL) at 37°C in a humidified atmosphere of 5% CO<sub>2</sub> and 95% air. Cells were harvested after brief incubation in trypsin.

### 2.2. Chronic restraint stress model

Female BALB/c-nu mice (4-6 weeks old) were purchased from the Laboratory Animal Research Center of Hubei Province (Wuhan, Hubei, China), and housed in laminar air flow cabinets under pathogen-free conditions with a 12-h light/12-h dark schedule and fed autoclaved standard chow and water. The research protocol was in accordance with the institutional guidelines of the Animal Care and Use Committee.

Mice were randomly divided into stress and control groups after a week in the new environment (six mice per group). Mice in the control group were allowed freedom of action throughout the experiment. For the chronic restraint stress group, each mouse was subjected to an established chronic physical restraint protocol (10,11), in which the mouse was restrained for 6 h daily (from 11 a.m. to 5 p.m.) in a 50 mL conical centrifuge tube filled with multiple punctures to allow ventilation. The mice were neither physically compressed nor experiencing pain. For both groups, SKOV-3 cells ( $2 \times 10^7$ ) were suspended in

100  $\mu$ L of Matrigel (Collaborative Biomedical, Bedford, USA) and were injected subcutaneously into the right lateral chest wall in close proximity to the axilla on day 8 after starting the experiment. All the mice were kept according to the protocol for 35 consecutive days after tumor cells implantation. Tumors were measured using callipers and volumes were approximated by the formula,  $\text{volume} = 1/6\pi ab^2$ , where  $a$  and  $b$  represent two perpendicular tumor diameters (12). Blood was drawn from the postorbital venous plexus of the mice for hematological analysis as described below. Mice in each group were sacrificed by cervical dislocation at the end of the experiment. Tumors were removed, weighed, and then stored at  $-80^\circ\text{C}$  for further analysis. Tumor growth inhibition rates were defined as a percentage of the control tumor weight.

### 2.3. Serum NE and IL-10 assay

Blood samples were centrifuged at 3,000 rpm for 10 min immediately after collection, and plasma was frozen until analysis. The serum NE and IL-10 levels were determined using Mouse NE (Wuhan Youersheng Technology Co., Ltd., Wuhan, Hubei, China) and IL-10 (Wuhan Boster Biological Engineering Co., Ltd., Wuhan, Hubei, China) ELISA kits, respectively, according to the manual instructions.

### 2.4. Protein extraction

Frozen xenograft tissue samples were homogenized on ice using a glass tissue grinder. For every 100 mg tissue, 1 mL lysis buffer (consisting of 40 mmol/L tris buffer (pH 7.5), 7 mol/L urea, 2 mol/L thiourea, 1% dithiothreitol, 4% 3-[3-(cholamidopropyl) dimethylammonio]-1-propanesulfonate (CHAPS), and 1 mmol/L ethylenediaminetetraacetic acid (EDTA)) and 10  $\mu$ L protease inhibitor cocktail were added. The homogenates were sonicated on ice using a sonifier (Sonoiprep150, SANYO Electric Co., Ltd., Moriguchi, Osaka, Japan). After sonication, 5  $\mu$ L (10  $\mu$ g/ $\mu$ L) DNase and 5  $\mu$ L (10  $\mu$ g/ $\mu$ L) RNase were added. Subsequently, the sample was incubated for 20 min on ice. Cellular debris was removed by centrifugation at 14,000 rpm/min for 20 min at 4°C, and the supernatants were collected. The protein concentrations were quantified by the Bradford protein assay. The obtained protein samples were sub-packaged, labeled, and stored at  $-80^\circ\text{C}$ .

### 2.5. Two-dimensional electrophoresis (2-DE)

Protein samples (100  $\mu$ g) were mixed with rehydration solution (8 mol/L urea, 2% CHAPS, 0.5% IPG buffer, 18 mmol/L DTT and a trace of bromophenol blue) to a volume of 350  $\mu$ L. This sample was loaded into strip holders together with 18 cm Immobiline DryStrips (linear pH gradient from pH 3 to 10), and the loaded strips were

covered with Drystrip Cover Fluid. The rehydration holders were placed in the IPGphor isoelectric focusing electrophoresis (IEF) system for passive rehydration for 12 h at 30 V at 20°C. Subsequently, isoelectric focusing of the first dimension was carried out. The proteins were focused at 20°C for 1 h at 500 V, then 1 h at 1,000 V, and finally 6 h at 8,000 V. After completion of the IEF program, the strips were equilibrated at room temperature in two steps: 15 min in an IPG equilibration buffer (50 mmol/L Tris-HCl solution (pH 8.8), 6 mol/L urea, 30% glycerol, 2% sodium dodecyl sulfate (SDS), and a trace of bromophenol blue) plus 1% DTT, followed by 15 min in IPG equilibration buffer plus 2.5% iodoacetamide (IAA). For the second dimension, SDS-PAGE with a 13% polyacrylamide gel was used. The IPG strips were placed on the top of the gel and the proteins were then separated according to their molecular weights. Electrophoresis was carried out at 20°C, 15 mA/gel for 15 min, followed by a 6 h run at 30 mA/gel until the bromophenol blue indicator front reached the bottom of the gels. Three 2-DE gels were performed for each group.

#### 2.6. Gel scanning and image analysis

After silver staining, the two-dimensional gels were imaged on an image scanner in a transmission mode, and quantitative analyses of the digitized images were performed using the Image Master 2D Platinum™ software (Amersham Pharmacia Biotech, Amersham, UK) according to the protocols provided by the manufacturer, which included background subtraction, spot detection, defining landmark annotations, and matching. The intensity of each spot was normalized to the total valid spot intensity. Gels from the control and stress group were analyzed simultaneously. Each sample was analyzed based on triplicate gels produced in identical conditions to demonstrate reproducibility and diminish experimental errors. An average gel would be selected as a standard gel in each group by matching analysis, with more homogeneous spots, fewer impurities and better representation of the spot distribution. Using image analysis software, target spots were compared to the average gel to detect increases/decreases in expression (to more than double/half that of control, respectively), and to catalogue significant inter-group variations.

#### 2.7. Protein identification by ultra performance liquid chromatography-electrospray tandem mass spectrometry (nanoUPLC-ESI-MS/MS)

Considering its compatibility to nanoUPLC-ESI-MS/MS analysis, we chose Coomassie Brilliant Blue G-250 staining in this study. We selected the preparative gels to perform Coomassie Brilliant Blue G-250 staining. Differentially expressed protein spots were selected, which were chosen according to the spots of silver staining gels. The spots were carefully excised from gels

using a biopsy scalpel, and spot pieces were digested with trypsin in a 1.5 mL siliconized Eppendorf tube. Spot pieces were washed twice with Milli-Q water, destained in 50% acetonitrile containing 100 mmol/L ammonium bicarbonate for 20 min at room temperature, dehydrated and dried using a vacuum centrifuge. The dried gel pieces were incubated in 50 mmol/L ammonium bicarbonate containing 0.1 µg/µL modified trypsin for digestion at 37°C overnight (12-16 h). The resulting harvested peptide mixture was prepared as a sample solution as described previously (13). Sample solution (5 µL) was injected into a nano-Acquity system and subjected to nanoUPLC-ESI-MS/MS analysis. The UPLC-ESI-MS/MS system consists of a nano-ACQUITY UPLC system and a Synapt high definition mass spectrometer using an electrospray ionization source Z-spray. The ACQUITY UPLC analytical column uses a 75 µm × 250 mm BEH C18 column packed with 1.7 µm particles, and the enrichment column is a 180 µm × 20 mm symmetry C18 packed with 5 µm particles. The column temperature was maintained at 35°C. Optimum separation was achieved with a gradient mobile phase (which flowed at a rate of 200 nL/min) and two mobile phases consisting of 0.1% formic acid in water and 0.1% formic acid in acetonitrile. The gradient conditions were 80 min 1-40% B, 10 min 40-80% B, 10 min 80% B, and 20 min 100% B, then a return to initial conditions. For ESI-MS/MS, ionization was achieved by using nano-electrospray ionization positive ions with a capillary voltage of 2.5 kV and a cone voltage of 35 V, the source temperature and desolvation temperature were set at 90 and 300°C, respectively. Nitrogen was used as the cone gas and for desolvation, with a flow rate of 50 and 500 L/h, respectively. Argon was used as the collision gas set at  $2.5 \times 10^{-3}$  mbar. Data were acquired in data dependent acquisition (DDA) mode, and the two highest intensity ions were selected from each scan, which was carried out using tandem mass spectrometry. MS/MS spectra were processed using total data acquisition software (PLGS, v2.3), and then analyzed with the Mascot search engine ([www.matrixscience.com](http://www.matrixscience.com)) against the NCBI nr database including two variable modifications: Carbamidomethyl (C) and Oxidation (M). One missed cleavage site was allowed for trypsin digestion, all mass values were considered monoisotopic, and the MS/MS tolerance was set at ±0.2 Da. Individual ion scores of > 38 indicate identity or extensive homology ( $p < 0.05$ ).

#### 2.8. Western blot analysis

For Western blotting, the method was essentially as previously described (14-16). Briefly, protein extracts were separated on SDS-PAGE and then blotted to polyvinylidene difluoride (PVDF) membranes (Millipore, USA). After incubating for 1 h with PBS containing 0.1% Tween 20 and 5% non-fat dried milk, primary antibodies were added and the membrane was incubated at room temperature

overnight. Primary antibodies in this study were rabbit anti-NDRG1 (Millipore, USA), and mouse anti-nm23 (Beijing Biosynthesis Biotechnology Co., Ltd., Beijing, China). After washing, goat anti-rabbit and goat anti-mouse horseradish peroxidase-conjugated second antibody were added, depending on the species of the primary antibody. After incubation for 1 h, membranes were decolorized with phosphate buffered saline (PBS) at room temperature, subjected to enhanced chemiluminescence, and exposed to film. The exposed films were examined visually and photographed or scanned.

### 2.9. Statistical analysis

Data was described as the mean  $\pm$  SD, and analyzed by Student's two-tailed *t*-test. The limit of statistical significance was  $p < 0.05$ . Statistical analysis was done with SPSS/Win17.0 software (SPSS, Inc., Chicago, IL, USA).

## 3. Results

### 3.1. Chronic restraint stress enhanced tumor growth

Mice in the stress group generally manifested as hyperactive with biting of the restraint tube for the first several days, indicating that they were in a state of dysphoria and anxiety. These manifestations were moderately improved in the subsequent days until the end of the experiment. Tumor nodules that were palpable appeared at about the fourth day after subcutaneous inoculation of SKOV-3 cells and started to grow quickly approximately at the ninth day in both groups. However, the growth of xenografts in the stress group showed a more rapid trend than that in the control group (Figure 1). Tumor volumes measured in the stress group were obviously larger than those in the control group at the

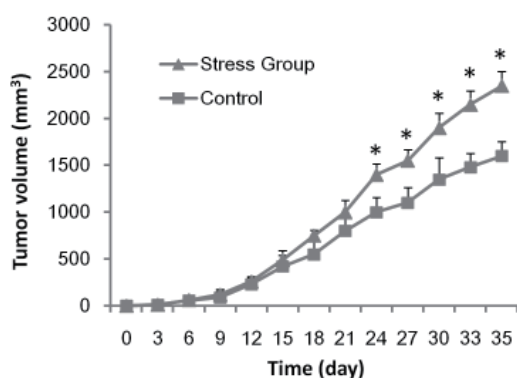


**Figure 1. Tumor volumes measured in the stress group and control.** SKOV-3 cells were inoculated into the mice 7 days after initiation of stress and were allowed to grow in nude mice for 35 days. Tumor volumes measured at a 3 day interval until the end of the experiment. The growth of SKOV-3 xenografts in stress group demonstrated a more rapid trend compared to control. \*  $p < 0.05$ , stress group vs. control.

time points of 24, 27, 30, 33, and 35 days ( $p < 0.05$  at each indicated time point). The SKOV-3 xenografts were removed after the experiment and weighed  $1.717 \pm 0.571$  g and  $1.083 \pm 0.286$  g for the stress group and control group, respectively, indicating that the chronic restraint stress significantly enhanced tumor growth ( $p < 0.05$ ).

### 3.2. Chronic restraint stress increased serum levels of NE and IL-10

Blood samples of mice in both the control and stress groups were obtained and centrifuged. The supernatant serum was subjected to ELISA assays for determination of NE and IL-10. NE concentrations of the stress and control group were measured at  $315.95 \pm 55.87$  and  $199.18 \pm 27.96$  ng/mL, respectively. There is a significant difference in NE concentration between the two groups ( $p < 0.01$ ). The serum level of IL-10 in the stress group was determined at  $240.03 \pm 22.25$  pg/mL, which is also obviously higher than that ( $201.08 \pm 21.30$  pg/mL) in the control group ( $p < 0.05$ ). These results indicated chronic restraint stress increased the serum levels of both NE and IL-10 in mice (Figure 2).

### 3.3. 2-DE map of SKOV-3 xenografts after exposure to chronic restraint stress

Proteins extracted from SKOV-3 xenografts were separated using 2-DE. Similar patterns of protein expression were detected in the tumor tissues from control and chronic restraint stress treated mice. On average, 1,400 protein spots were detected per gel in the stress and control group. Nineteen protein spots showed a significant difference in expression levels between the stress group and control ( $p < 0.05$ ), including 14 spots that were upregulated, 4 spots that were downregulated, and 1 spot that was only detected in the stress group. The spots were all distributed between pI of 4-10 and molecular weight (MW) of 14-60 kDa. Among these differential staining spots, the expression levels in two spots (designated names S7121 and S5543) positioned

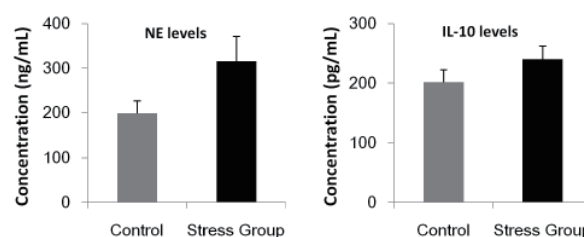


**Figure 2. NE and IL-10 levels determined in the stress group and control.** The mice in the stress group were immobilized 6 h daily for a total of 42 days with a restraint system. Blood samples were obtained at the end of the experiment and serum concentrations of NE and IL-10 were determined using ELISA. Chronic stress significantly increased the serum levels of NE and IL-10 compared to control. \*  $p < 0.05$ , \*\*  $p < 0.01$ , stress group vs. control.



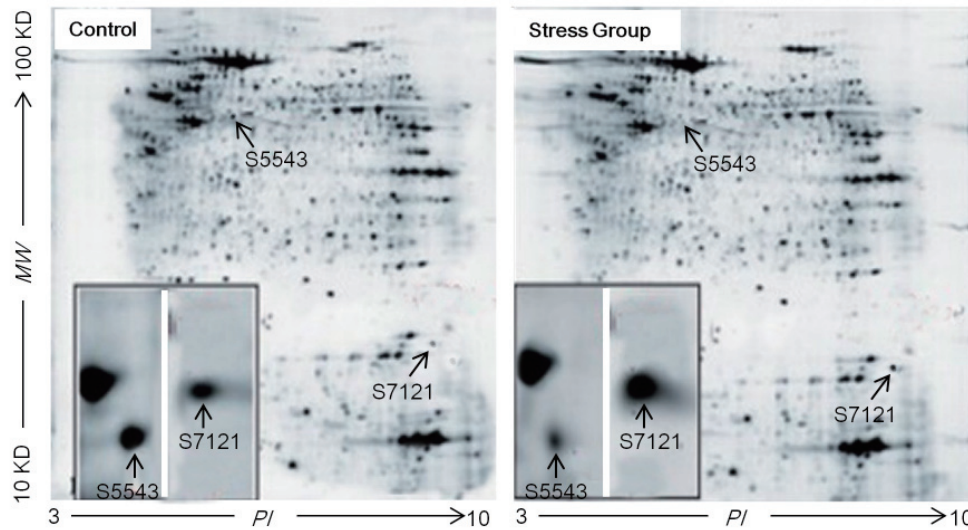


**Figure 3. 2-DE maps of SKOV-3 xenografts in the stress group and control.** Tumor tissues were removed at the end of experiment and subjected to 2-DE. After silver staining, the two-dimensional gels were imaged on an image scanner in a transmission mode, and quantitative analyses of the digitized images were performed. Protein S7121 (pI 7.1, MW 21 kDa) was significantly upregulated while protein S5543 (pI 5.5, MW 43 kDa) was obviously downregulated in tumor tissues of stress group.

**Table 1. NanoUPLC-ESI-MS/MS analyses of nm23 and NDRG1 in SKOV-3 xenografts**

Protein name	Nominal mass (Mr)/ calculated PI value	Score <sup>a</sup>	Sequence coverage (%)	Change in expression <sup>b</sup>	Change-fold (mean $\pm$ SD)	<i>p</i> -value <sup>c</sup>
nm23	20398/7.1	349	33	Up	2.28 $\pm$ 0.16	< 0.05
NDRG1	42808/5.5	736	36	Down	-(2.42 $\pm$ 0.17)	< 0.05

<sup>a</sup> Individual ions scores > 38 indicate identity or extensive homology. <sup>b</sup> Up- or down-regulated in the stress group vs. the control group. <sup>c</sup> Data were analyzed with an independent Student's *t*-test with SPSS version 17.0 software. Differences was considered significant if *p* < 0.05.

at pI 7.1, MW 21 kDa and pI 5.5, MW 43 kDa were profoundly different between the two groups (Figure 3). Expression level of protein S7121 in the stress group was up-regulated and was shown to be 2.2-fold over that in the control. On the contrary, expression level of protein S5543 in the stress group was down-regulated and was about 0.4-fold over that in the control. These results suggested chronic restraint stress altered protein expression profiles in SKOV-3 xenografts.

#### 3.4. Identification of differentially expressed proteins in SKOV-3 xenografts

To identify differentially expressed proteins in the xenografts after exposure of chronic restraint stress, protein spots S7121 and S5543 were excised from 2-DE gels, and then subjected to nanoUPLC-ESI-MS/MS analysis. Proteins S7121 and S5543 were identified as nm23 and NDRG1 by searching the NCBI database. An overview of these two proteins is presented in Table 1.

In order to verify the results of proteomic analyses, tumor tissues from both groups were grinded and total proteins were extracted and subjected to Western blotting

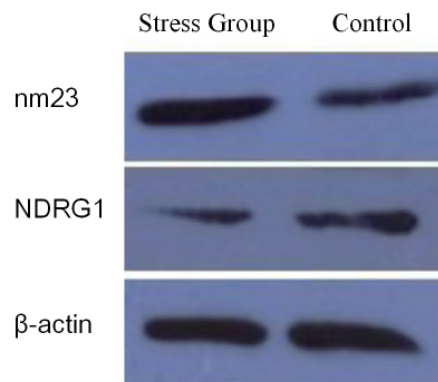


**Figure 4. Western blot analyses of nm23 and NDRG1 expression in SKOV-3 xenografts.** Compared to control, nm23 expression is increased while NDRG1 expression is downregulated in the stress group.

analysis. As shown in Figure 4, the average band intensity of nm23 in the stress group was increased compared to control, whereas the signal of NDRG1 was decreased in this group. These results indicated that expression of nm23 was enhanced and expression of NDRG1 was reduced after exposure to chronic restraint stress, which were in agreement with the results of proteomic analyses.

#### 4. Discussion

The current study used an established ectopic mouse model in which human ovarian carcinoma cells SKOV-3 were subcutaneously inoculated into the right lateral chest wall in close proximity to the axilla of nude mice. We experimentally stressed animals 6 h daily for a total of 42 days with a physical restraint system, in which periodic immobilization is supposed to induce high levels of SNS and HPA activity characteristic of chronic stress. We examined the effects of stress on the growth of tumor cells which were inoculated 7 days after the initiation of stress. In mice exposed to stress, mean tumor weight increased by 71.7% compared to control. We found that serum levels of NE and IL-10 were obviously increased in the mice receiving stress. Furthermore, we demonstrated that two proteins nm23 and NDRG1 were differentially expressed in tumor tissues in the stress group. These results suggested that alteration of serum levels of NE and IL-10 and tissue expressions of nm23 and NDRG1 may be involved in the effects of chronic stress in promoting the growth of ovarian carcinoma.

Previous studies suggested that changes in stress-related neuroendocrine transmitters such as NE during psychological stress lead to a modulation of immune cells and tumor microenvironment (8). Mechanisms underlying modulation of the immune function by NE were demonstrated that adrenergic receptors in immune cells bind NE to activate the cAMP response element-binding protein (CREB), which in turn induces the transcription of genes encoding for a variety of cytokines such as IL-10 (17-20). IL-10 is an immunosuppressive cytokine that has a variety of inhibition effects on the anti-tumor immune response such as reducing macrophage inflammatory response (21). Besides those indirect antitumor effects by NE through suppressing the immune function of organisms, research has recognized that NE could exhibit direct influence on tumor progression and this effect was mainly through NE and the  $\beta$ -adrenergic receptor ( $\beta$ -AR) signal pathway in cancer cells (7,9,22-23).  $\beta$ -AR signals can activate several common intracellular proliferative and pro-migratory signaling pathways, such as the cAMP/PKA, the mitogen-activated protein kinase (MAPK)/extracellular signal-regulated kinase (ERK1/2) and phosphatidylinositol-3-kinase (PI3K)/AKT signaling pathways (24,25). Thus, the total effects of psychological stress converging on ovarian cancer cells observed in our study are probably mediated by indirect immune suppression and direct tumor promotion processes.

We further explored the changes in protein expression in ovarian carcinoma after receiving chronic psychological stress and found that the stress altered the protein expression profiles of tumor tissues. Among a series of differentially expressed

proteins, levels of two proteins which were identified as nm23 and NDRG1 were profoundly different between the stress group and control. We found that nm23 was significantly upregulated while NDRG1 was obviously downregulated in tumor tissues when the mice were exposed to stress. The *nm23* gene is a putative metastasis-suppressor gene that was originally identified by screening of cDNA libraries from murine melanoma cell sublines of varying metastatic potential (26). However, subsequent studies showed that this protein plays controversial or tissue-specific roles in cancer progression (27,32). In ovarian carcinoma, evidence in favor of its role in promoting tumor progression were reported (33,34). These studies suggested that nm23 has a biological function that leads to poor clinical outcomes in ovarian carcinoma. In light of those findings, upregulation of nm23 may contribute to the effects of chronic stress in stimulating the growth of ovarian carcinoma. Another protein NDRG1 that was found significantly downregulated in stress-imposed tumor tissue is encoded by the gene belonging to the N-myc downregulated gene family. NDRG1 is a cytoplasmic protein involved in stress responses, hormone responses, cell growth, and differentiation (35,36). Studies demonstrated that NDRG1 expression was decreased in cancer primary and metastatic cells when compared to normal cells and was thought to function as a metastasis suppressor in cancer types including ovarian, colon, and prostate cancers (37-39). NDRG1 has also been reported to be necessary for p53-mediated apoptosis and it plays a role in suppressing malignant cell growth (40). Thus, the stimulatory effects of chronic stress on the growth of ovarian carcinoma may also be partially ascribed to decreased expression of NDRG1 in tumor tissues.

In conclusion, the current study confirmed that chronic psychological stress exhibited an adverse effect on the progression of ovarian carcinoma in a mouse model. Mechanisms underlying this effect were revealed to be related to increasing the serum levels of NE and IL-10 in the mice as well as upregulating and downregulating the expression of a tumor promoting protein nm23 and a tumor suppressing protein NDRG1, respectively, in ovarian carcinoma tissues. Evidence provided in this study should help further understanding of the molecular mechanisms of the adverse effects of psychological stress on the progression of ovarian carcinoma and designing corresponding strategies to cope with this disease.

#### References

1. GLOBOCAN 2008. World Health Organization. <http://globocan.iarc.fr/> (accessed December 21, 2012).
2. Mandic A, Tesic M, Vujkov T, Novta N, Rajovic J. Ovarian cancer stage III/IV: Poor prognostic factors. Arch of Oncol. 2001; 9:13-16.
3. Li Z, Zhao X, Yang J, Wei Y. Proteomics profile changes

- in cisplatin-treated human ovarian cancer cell strain. *Sci China C Life Sci.* 2005; 48:648-657.
4. De Marco C, Rinaldo N, Bruni P, Malzoni C, Zullo F, Fabiani F, Losito S, Scrima M, Marino FZ, Franco R, Quintiero A, Agosti V, Viglietto G. Multiple genetic alterations within the PI3K pathway are responsible for AKT activation in patients with ovarian carcinoma. *PLoS One.* 2013; 8:e55362.
  5. Garssen B. Psychological factors and cancer development: evidence after 30 years of research. *Clin Psychol Rev.* 2004; 24:315-338.
  6. Chida Y, Hamer M, Wardle J, Steptoe A. Do stress-related psychosocial factors contribute to cancer incidence and survival? *Nat Clin Pract Oncol.* 2008; 5:466-475.
  7. Sood AK, Bhatti R, Kamat AA, Landen CN, Han L, Thaker PH, Li Y, Gershenson DM, Lutgendorf S, Cole SW. Stress hormone-mediated invasion of ovarian cancer cells. *Clin Cancer Res.* 2006; 12:369-375.
  8. Yuan A, Wang S, Li Z, Huang C. Psychological aspect of cancer: From stressor to cancer progression. *Exp Ther Med.* 2010; 1:13-18.
  9. Thaker PH, Han LY, Kamat AA, *et al.* Chronic stress promotes tumor growth and angiogenesis in a mouse model of ovarian carcinoma. *Nat Med.* 2006; 12:939-944.
  10. Alfonso J, Frick LR, Silberman DM, Palumbo ML, Genaro AM, Frasch AC. Regulation of hippocampal gene expression is conserved in two species subjected to different stressors and antidepressant treatments. *Biol Psychiatry.* 2006; 59:244-251.
  11. Sheridan JF, Dobbs C, Jung J, Chu X, Konstantinos A, Padgett D, Glaser R. Stress-induced neuroendocrine modulation of viral pathogenesis and immunity. *Ann N Y Acad Sci.* 1998; 840:803-808.
  12. Shi W, Siemann DW. Inhibition of renal cell carcinoma angiogenesis and growth by antisense oligonucleotides targeting vascular endothelial growth factor. *Br J Cancer.* 2002; 87:119-126.
  13. Winter D, Kugelstadt D, Seidler J, Kappes B, Lehmann WD. Protein phosphorylation influences proteolytic cleavage and kinase substrate properties exemplified by analysis of *in vitro* phosphorylated *Plasmodium falciparum* glideosome-associated protein 45 by nano-ultra performance liquid chromatography-tandem mass spectrometry. *Anal Biochem.* 2009; 393:41-47.
  14. Kandala PK, Srivastava SK. Regulation of Janus-activated kinase-2 (JAK2) by diindolylmethane in ovarian cancer *in vitro* and *in vivo*. *Drug Discov Ther.* 2012; 6:94-101.
  15. Bao GY, Wang HZ, Shang YJ, Fan HJ, Gu ML, Xia R, Qin Q, Deng AM. Quantitative proteomic study identified cathepsin B associated with doxorubicin-induced damage in H9c2 cardiomyocytes. *Biosci Trends.* 2012; 6:283-287.
  16. An YT, Zhao Z, Sheng YC, Min Y, Xia YY. Therapeutic time window of YGY-E neuroprotection of cerebral ischemic injury in rats. *Drug Discov Ther.* 2011; 5:76-83.
  17. Glaser R, Kiecolt-Glaser JK. Stress-induced immune dysfunction: Implications for health. *Nat Rev Immunol.* 2005; 5:243-251.
  18. Reiche EM, Nunes SO, Morimoto HK. Stress, depression, the immune system, and cancer. *Lancet Oncol.* 2004; 5:617-625.
  19. Padgett DA, Glaser R. How stress influences the immune response. *Trends Immunol.* 2003; 24:444-448.
  20. Segerstrom SC, Miller GE. Psychological stress and the human immune system: A meta-analytic study of 30 years of inquiry. *Psychol Bull.* 2004; 130:601-630.
  21. Sato T, Terai M, Tamura Y, Alexeev V, Mastrangelo MJ, Selvan SR. Interleukin 10 in the tumor microenvironment: A target for anticancer immunotherapy. *Immunol Res.* 2011; 51:170-182.
  22. Antoni MH, Lutgendorf SK, Cole SW, Dhabhar FS, Sephton SE, McDonald PG, Stefanek M, Sood AK. The influence of bio-behavioural factors on tumour biology: Pathways and mechanisms. *Nat Rev Cancer.* 2006; 6:240-248.
  23. Lutgendorf SK, Cole S, Costanzo E, Bradley S, Coffin J, Jabbari S, Rainwater K, Ritchie JM, Yang M, Sood AK. Stress-related mediators stimulate vascular endothelial growth factor secretion by two ovarian cancer cell lines. *Clin Cancer Res.* 2003; 9:4514-4521.
  24. Hall RA. Beta-adrenergic receptors and their interacting proteins. *Semin Cell Dev Biol.* 2004; 15:281-288.
  25. Dorsam RT, Gutkind JS. G-protein-coupled receptors and cancer. *Nat Rev Cancer.* 2007; 7:79-94.
  26. Steeg PS, Bevilacqua G, Kopper L, Thorgeirsson UP, Talmadge JE, Liotta LA, Sobel ME. Evidence for a novel gene associated with low tumor metastatic potential. *J Natl Cancer Inst.* 1988; 80:200-204.
  27. Florenes VA, Aamdal S, Myklebost O, Maelandsmo GM, Bruland OS, Fodstad O. Levels of nm23 messenger RNA in metastatic malignant melanomas: inverse correlation to disease progression. *Cancer Res.* 1992; 52:6088-6091.
  28. Nakayama T, Ohtsuru A, Nakao K, Shima M, Nakata K, Watanabe K, Ishii N, Kimura N, Nagataki S. Expression in human hepatocellular carcinoma of nucleoside diphosphate kinase, a homologue of the nm23 gene product. *J Natl Cancer Inst.* 1992; 84:1349-1354.
  29. Ozeki Y, Takishima K, Mamiya G. Immunohistochemical analysis of nm23/NDP kinase expression in human lung adenocarcinoma: association with tumor progression in Clara cell type. *Jpn J Cancer Res.* 1994; 85:840-846.
  30. Hailat N, Keim DR, Melhem RF, Zhu XX, Eckerskorn C, Brodeur GM, Reynolds CP, Seeger RC, Lottspeich F, Strahler JR, *et al.* High levels of p19/nm23 protein in neuroblastoma are associated with advanced stage disease and with N-myc gene amplification. *J Clin Invest.* 1991; 88:341-345.
  31. Leone A, Flatow U, VanHoutte K, Steeg PS. Transfection of human nm23-H1 into the human MDA-MB-435 breast carcinoma cell line: Effects on tumor metastatic potential, colonization and enzymatic activity. *Oncogene.* 1993; 8:2325-2333.
  32. Royds JA, Cross SS, Silcocks PB, Scholefield JH, Rees RC, Stephenson TJ. Nm23 'anti-metastatic' gene product expression in colorectal carcinoma. *J Pathol.* 1994; 172:261-266.
  33. Youn BS, Kim DS, Kim JW, Kim YT, Kang S, Cho NH. Nm23 as a prognostic biomarker in ovarian serous carcinoma. *Mod Pathol.* 2008; 21:885-892.
  34. Schneider J, Pollan M, Jimenez E, Marenbach K, Martinez N, Volm M, Marx D, Meden H. nm23-H1 expression defines a high-risk subpopulation of patients with early-stage epithelial ovarian carcinoma. *Br J Cancer.* 2000; 82:1662-1670.
  35. Okuda T, Kokame K, Miyata T. Functional analyses of NDRG1, a stress-responsive gene. *Seikagaku.* 2005; 77:630-634.
  36. Melotte V, Qu X, Ongenaert M, van Criekinge W, de

- Bruine AP, Baldwin HS, van Engeland M. The N-myc downstream regulated gene (NDRG) family: Diverse functions, multiple applications. *FASEB J.* 2010; 24:4153-4166.
37. Zhao G, Chen J, Deng Y, Gao F, Zhu J, Feng Z, Lv X, Zhao Z. Identification of NDRG1-regulated genes associated with invasive potential in cervical and ovarian cancer cells. *Biochem Biophys Res Commun.* 2011; 408:154-159.
38. Guan RJ, Ford HL, Fu Y, Li Y, Shaw LM, Pardee AB. Drg-1 as a differentiation-related, putative metastatic suppressor gene in human colon cancer. *Cancer Res.* 2000; 60:749-755.
39. Bandyopadhyay S, Pai SK, Gross SC, Hirota S, Hosobe S, Miura K, Saito K, Commes T, Hayashi S, Watabe M, Watabe K. The Drg-1 gene suppresses tumor metastasis in prostate cancer. *Cancer Res.* 2003; 63:1731-1736.
40. Ellen TP, Ke Q, Zhang P, Costa M. NDRG1, a growth and cancer related gene: regulation of gene expression and function in normal and disease states. *Carcinogenesis.* 2008; 29:2-8.
- (Received January 21, 2013; Revised February 25, 2013; Accepted February 26, 2013)*